

Green's Function Reaction Dynamics: a new approach to simulate biochemical networks at the particle level and in time and space

Jeroen S. van Zon¹ and Pieter Rein ten Wolde^{2,1}

¹*Division of Physics and Astronomy, Vrije Universiteit,
De Boelelaan 1081, 1081 HV Amsterdam, The Netherlands.*

²*FOM Institute for Atomic and Molecular Physics,
Kruislaan 407, 1098 SJ Amsterdam, The Netherlands.*

(Dated: October 25, 2018)

Biochemical networks are the analog computers of life. They allow living cells to control a large number of biological processes, such as gene expression and cell signalling. In biochemical networks, the concentrations of the components are often low. This means that the discrete nature of the reactants and the stochastic character of their interactions have to be taken into account. Moreover, the spatial distribution of the components can be of crucial importance. However, the current numerical techniques for simulating biochemical networks either ignore the particulate nature of matter or treat the spatial fluctuations in a mean-field manner. We have developed a new technique, called Green's Function Reaction Dynamics (GFRD), that makes it possible to simulate biochemical networks at the particle level and in both time and space. In this scheme, a maximum time step is chosen such that only single particles or pairs of particles have to be considered. For these particles, the Smoluchowski equation can be solved analytically using Green's functions. The main idea of GFRD is to exploit the exact solution of the Smoluchowski equation to set up an event-driven algorithm. This allows GFRD to make large jumps in time when the particles are far apart from each other. Here, we apply the technique to a simple model of gene expression. The simulations reveal that the scheme is highly efficient. Under biologically relevant conditions, GFRD is up to six orders of magnitude faster than conventional particle-based techniques for simulating biochemical networks in time and space.

PACS numbers: 87.16.Yc,87.16.Ac,2.70.-c,5.40.-a

I. INTRODUCTION

Organisms can be viewed as information processing machines. Even relatively simple organisms, such as the bacterium *Escherichia coli*, can perform fairly complex computations such as: **if lactose is present and not glucose is present, then use lactose**. Recent technological developments have made it possible to obtain information on the regulatory architecture of the cell on an unprecedented scale. In addition, extensive databases are now available that catalog biochemical pathways. Nevertheless, our understanding of the mechanisms that allow living cells to process information is still limited. One important reason for this is that these mechanisms are controlled by stochastic processes.

In the living cell, computations are performed by molecules that chemically and physically interact with each other. These components, that form what is called a biochemical network, behave stochastically. They often move in an erratic fashion, namely by diffusion, and act upon each other in a stochastic manner - chemical reactions, and equally important, physical interactions are probabilistic in nature. These factors become particularly important when the concentrations are low. In the living cell, this is often the case, and, as a result, biochemical networks can be highly stochastic [1, 2]. In this respect, it is a remarkable fact that many biological processes operate reliably with surprisingly small numbers of molecules.

Another important reason for our limited understanding of biochemical networks is that they operate not only in time, but also in space. In the living cell, signals often have to be transmitted from one place to the next by the diffusive motion of “messenger” molecules; their concentrations can be non-uniform, and more importantly, their low mobility can limit the response time of the network. Moreover, many processes, such as the immune response, involve a complex spatial reorganization of the reactants. Finally, a large number of biological activities require the localized assembly of a complex of proteins. All these processes can only be accurately investigated using techniques that resolve the network in time and space.

In principle, computer simulations are ideally suited for studying how biochemical networks reliably process information in time and space. However, the current numerical techniques are of limited use for this purpose. Table I gives an overview of the commonly used techniques for analysing biochemical networks. The conventional approach is to write down the macroscopic rate equations and to solve the corresponding differential equations numerically. In this method, the evolution of the network is deterministic. It is implicitly assumed that the concentrations are large and that fluctuations can be neglected. The effect of fluctuations is often included by adding a noise term to the macroscopic rate equations [3]. However, at low concentrations, this approach is bound to fail, as demonstrated by Togashi and Kaneko [4] and

Shnerb and coworkers [5]. At low concentrations, we have to recognize the discrete nature of the reactants and the stochastic character of their interactions. Currently, two techniques exist for simulating biochemical networks at the particle level [6, 7]. Both of these are consistent with the chemical master equation. However, the chemical master equation relies on the assumption that there are many non-reactive collisions to stir the system between the reactive collisions. In effect, it is implicitly assumed that at each instant the particles are uniformly distributed in space. This is a serious limitation. As discussed above, the functioning of many biochemical networks depends crucially on their spatial organization. Moreover, fluctuations of the components in space can be a major source of noise in biochemical networks.

Clearly, in many cases we have to describe biochemical networks both temporally and spatially at the molecular level. However, the current techniques for simulating biochemical networks cannot accomplish this since they either ignore the particulate nature of matter, or treat the spatial fluctuations in a mean-field manner. We have developed a new technique, named Green's Function Reaction Dynamics (GFRD), that makes it possible to simulate biochemical networks at the particle level and in time and space. This technique, which we describe in detail in the next section, is an event-driven algorithm in which the particles are propagated in space between reaction events using Green's functions. In the subsequent section, we apply GFRD to a simple model of gene expression. The calculations show that the technique is highly efficient. We thus believe that GFRD brings simulating biochemical networks at the particle level and in time and space within reach.

II. NUMERICAL TECHNIQUE

A. Introduction

In this section we discuss the main ideas underlying Green's Function Reaction Dynamics (GFRD). GFRD is a stochastic scheme that combines the propagation of the particles in space with the reactions between them in an efficient manner. Most proteins are believed to be transported by their diffusive motion, although in eukaryotic cells, cytoskeletal networks and motor proteins may facilitate the transport of molecules [8]. Such mechanisms of active transport have not been observed in bacteria, where diffusion is believed to be the primary means of intracellular movement. For now, we will assume that the network components are transported by diffusion, although the technique could be extended to include active transport as well.

Two approaches seem to be potentially useful for simulating biochemical networks at the particle level and in time and space. The first is to let the particles undergo a random walk on a lattice and to let reaction partners react with a certain probability when they happen to meet

each other. This technique has a number of limitations, the most important of which are that the physical dimensions of the particles and the interactions between them cannot conveniently be described.

Brownian Dynamics is a more appealing technique. This is a stochastic dynamics scheme, in which the particles are propagated in space according to the overdamped limit of the Langevin equation. In Brownian Dynamics, the solvent is considered implicitly; only the solute particles are considered explicitly. The forces experienced by these particles contain two parts: a conservative part, which arises from the interactions with the other solute particles, and a random part. The latter is the dynamical remnant of the solvent - the solutes are thought to experience random forces from the solvent. Via the fluctuation-dissipation theorem and the Einstein relation, the random forces are related to the diffusion constant of the particles. To be more explicit, the equations of motion for the solute particles are given by:

$$\dot{\mathbf{r}}_s = \frac{D_s}{k_B T} (\mathbf{F}_s + \delta\mathbf{F}_s). \quad (1)$$

Here, \mathbf{r}_s denotes the position of solute particle s , D_s is the diffusion constant of solute particle s , $k_B T$ is Boltzmann's constant times temperature, \mathbf{F}_s is the conservative force exerted by the other solute particles, and $\delta\mathbf{F}_s$ is the random force that arises from the interactions with the solvent.

Brownian Dynamics has a number of advantages over lattice-based techniques: the particles move in continuum space; the interactions between particles - the potential of mean force - can easily be described; excluded volume effects are taken into account naturally; and a different diffusion constant can be assigned to each type of particles.

In principle, chemical reactions can be straightforwardly implemented into the Brownian Dynamics scheme: the particles are propagated according to Eq. (1) and when two reaction partners happen to meet each other, they can react with a probability that is consistent with the rate constant. However, the major drawback of such a scheme is that very small time steps are needed in order to resolve the collision events. This makes brute-force Brownian Dynamics a very inefficient scheme to simulate biochemical networks.

The main idea of GFRD is to combine in one step the propagation of the particles in space with the reactions between them. To see how this can be accomplished, one should realize that Brownian Dynamics is, in effect, a *numerical* procedure for solving the Smoluchowski equation [9]. However, for a pair of particles, that not only move diffusively, but also can react according to $A + B \rightarrow C + D + \dots$, the Smoluchowski equation can be solved *analytically* using Green's functions. The Green's function for the pair of particles A and B , $p(\mathbf{r}, t | \mathbf{r}_0, t_0)$, yields the probability that the interparticle vector \mathbf{r}_0 at time t_0 becomes \mathbf{r} at a later time t . The essence of GFRD is to exploit this exact solution for

Description		Accounts for spatial extent of network	Incorporates fluctuations
Continuum	Ordinary differential equations	No	No
	Stochastic differential equations	No	Only at high concentrations
	Reaction diffusion equations	Yes	No
Particle-based	Chemical master equation	No	Yes
	GFRD	Yes	Yes

TABLE I: Overview of the commonly used techniques and the newly developed technique, called Green’s Function Reaction Dynamics (GFRD), to simulate biochemical networks. GFRD takes both the discrete nature and the spatial distribution of the reactants into account.

a pair of particles to set up an event-driven algorithm. This allows GFRD to make large jumps in time when the particles are far apart from each other. In biochemical networks this is often the case as the reactant concentrations are usually low. GFRD is therefore ideally suited for biochemical networks. Below we describe the scheme in more detail.

B. Overview of the algorithm

Let us imagine a configuration of reactants as shown in Fig. 1. The circles indicate the distances the particles can travel in a time step Δt . For a particle that moves by free diffusion with a diffusion constant D , that distance scales as $\langle |\Delta \mathbf{r}|^2 \rangle \sim D\Delta t$. Intersecting circles represent particles that may meet within the time step Δt . Isolated particles and pairs of interacting particles can be propagated analytically using Green’s functions, as we will discuss in detail in the next section. Clearly, the larger the time step, the larger the circles and the greater the probability that reaction partners meet and react with each other. However, we cannot make the time step arbitrarily large: if a given particle can collide with more than one other particle during a time step, then propagating the particles becomes a many-body problem that we can not solve analytically. The size of a time step is thus limited by the requirement that each particle can interact with at most one other particle during that time step. This constraint sets an upper limit on the magnitude of a time step in our algorithm; we will call it Δt_{\max} . However, provided that we consider times Δt smaller than Δt_{\max} , the problem can be reduced to that of propagating single particles and pairs of particles. This can be solved analytically using Green’s functions, as we will now describe.

C. Monomolecular reactions - the Green’s function for single particles

In this section, we consider the propagation of a *single* particle. We assume that the particle is spherical in shape and moves by free diffusion with a diffusion constant D . The diffusive motion of the particle is described by the Einstein diffusion equation

$$\partial_t p_1(\mathbf{r}, t | \mathbf{r}_0, t_0) = D \nabla^2 p_1(\mathbf{r}, t | \mathbf{r}_0, t_0). \quad (2)$$

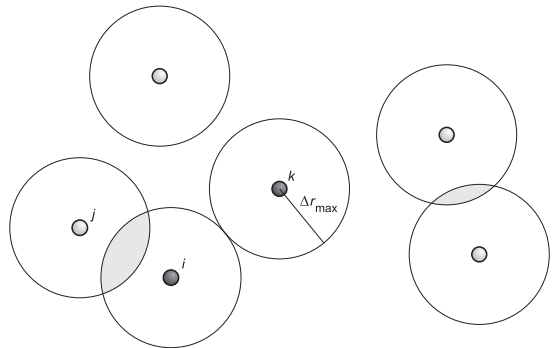


FIG. 1: Determination of the maximum time step, Δt_{\max} . The maximum size of the time step is set by the requirement that each particle can interact with at most one other particle during that time step; each particle i can thus travel a distance of at most $\Delta r_{\max, i}$ during a time step, as indicated by the circles. We have used the operational criterion $\Delta r_{\max, i} = H \sqrt{6D_i \Delta t_{\max, i}}$, with D_i being the diffusion constant of particle i . A value of $H = 3$ was found to yield a good conservation of the correct steady-state distribution. In this example, each particle is assumed to have the same diffusion constant; the time step is limited by the constraint that particles i and k should not interact as particle i can already interact with particle j . Note that with this maximum time step the many-body problem of propagating the N particles is reduced to that of propagating single particles and pairs of particles.

Here, $p_1(\mathbf{r}, t|\mathbf{r}_0, t_0)$ is the probability that the particle is at position \mathbf{r} at time t , given that it was at \mathbf{r}_0 at time t_0 . This diffusion equation can be solved subject to the initial condition and the boundary condition

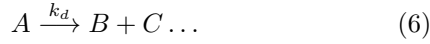
$$p_1(\mathbf{r}, t_0|\mathbf{r}_0, t_0) = \delta(\mathbf{r} - \mathbf{r}_0), \quad (3)$$

$$p_1(|\mathbf{r}| \rightarrow \infty, t|\mathbf{r}_0, t_0) = 0, \quad (4)$$

respectively. The solution $p_1(\mathbf{r}, t|\mathbf{r}_0, t_0)$ is known as a Green's function. It is given by the well-known expression

$$p_1(\mathbf{r}, t|\mathbf{r}_0, t_0) = \frac{1}{[4\pi D(t-t_0)]^{3/2}} \exp\left[-\frac{|\mathbf{r}-\mathbf{r}_0|^2}{4D(t-t_0)}\right]. \quad (5)$$

We now consider the case in which the particle does not only move diffusively, but also can "decay" according to



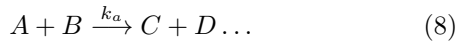
We will assume that, if the reaction happens, it happens *instantaneously*. This means that the reaction can be decoupled from the diffusive motion of the particle. If the reaction is a Poisson process with $k_d dt$ being the probability that a reaction occurs in an infinitesimal time interval dt , then the probability that the *next* reaction occurs between t and $t + dt$, is

$$q_d(t|t_0)dt = k_d \exp[-k_d(t-t_0)] dt. \quad (7)$$

In section IIE, we will use Eqs. 5 and 7 to set up an event-driven algorithm.

D. Bimolecular reactions - the Green's function for pairs of particles

In this section, we consider *one pair* of particles A and B that can react according to



We again assume that the particles A and B are spherical in shape and move by their diffusive motion; the diffusion constants for particle A and B are D_A and D_B , respectively. Furthermore, we assume that the particles react with an intrinsic rate constant k_a when they have approached each other within the reaction distance $\sigma = (d_A + d_B)/2$, where d_A and d_B are the diameters of particles A and B , respectively. In addition, we imagine that the particles interact with each other via a potential $U(\mathbf{r})$, where $\mathbf{r} = \mathbf{r}_B - \mathbf{r}_A$. The force acting on particle B is thus given by $-\nabla_B U(\mathbf{r}) = \mathbf{F}(\mathbf{r})$, while the force acting on particle A is given by $-\mathbf{F}(\mathbf{r})$.

We aim to derive the distribution function $p_2(\mathbf{r}_A, \mathbf{r}_B, t|\mathbf{r}_{A0}, \mathbf{r}_{B0}, t_0)$, which yields the probability that the particles A and B are at positions \mathbf{r}_A and \mathbf{r}_B at time t , given that they were at \mathbf{r}_{A0} and \mathbf{r}_{B0} at

time t_0 . This distribution function satisfies for $|\mathbf{r}| \geq \sigma$ the following Smoluchowski equation [9]

$$\begin{aligned} \partial_t p_2(\mathbf{r}_A, \mathbf{r}_B, t|\mathbf{r}_{A0}, \mathbf{r}_{B0}, t_0) = \\ [D_A \nabla_A^2 + D_B \nabla_B^2 - D_B \beta \nabla_B \cdot \mathbf{F}(\mathbf{r}) + D_A \beta \nabla_A \cdot \mathbf{F}(\mathbf{r})] \\ \times p_2(\mathbf{r}_A, \mathbf{r}_B, t|\mathbf{r}_{A0}, \mathbf{r}_{B0}, t_0). \end{aligned} \quad (9)$$

It will be convenient to make a coordinate transformation

$$\mathbf{R} = \sqrt{D_B/D_A} \mathbf{r}_A + \sqrt{D_A/D_B} \mathbf{r}_B, \quad (10)$$

$$\mathbf{r} = \mathbf{r}_B - \mathbf{r}_A, \quad (11)$$

and to define the operators

$$\nabla_{\mathbf{R}} = \partial/\partial \mathbf{R}, \quad (12)$$

$$\nabla_{\mathbf{r}} = \partial/\partial \mathbf{r}. \quad (13)$$

Eq. 9 can then be rewritten as:

$$\begin{aligned} \partial_t p_2(\mathbf{R}, \mathbf{r}, t|\mathbf{R}_0, \mathbf{r}_0, t_0) = (D_A + D_B)[\nabla_{\mathbf{R}}^2 + \nabla_{\mathbf{r}} \cdot (\nabla_{\mathbf{r}} - \mathbf{F}(\mathbf{r}))] \\ \times p_2(\mathbf{R}, \mathbf{r}, t|\mathbf{R}_0, \mathbf{r}_0, t_0), \\ |\mathbf{r}| \geq \sigma. \end{aligned} \quad (14)$$

It is seen that Eq. 14 describes two independent random processes - free diffusion in the coordinate \mathbf{R} and diffusion with a drift in the coordinate \mathbf{r} . This means that the distribution function $p_2(\mathbf{r}_A, \mathbf{r}_B, t|\mathbf{r}_{A0}, \mathbf{r}_{B0}, t_0)$ can be factorized as $p_2^{\mathbf{R}}(\mathbf{R}, t|\mathbf{R}_0, t_0)p_2^{\mathbf{r}}(\mathbf{r}, t|\mathbf{r}_0, t_0)$ and that the above equation can be reduced to one Smoluchowski equation for the coordinate \mathbf{R} and one for the coordinate \mathbf{r} :

$$\begin{aligned} \partial_t p_2^{\mathbf{R}}(\mathbf{R}, t|\mathbf{R}_0, t_0) = (D_A + D_B)\nabla_{\mathbf{R}}^2 \\ \times p_2^{\mathbf{R}}(\mathbf{R}, t|\mathbf{R}_0, t_0), \end{aligned} \quad (15)$$

$$\begin{aligned} \partial_t p_2^{\mathbf{r}}(\mathbf{r}, t|\mathbf{r}_0, t_0) = (D_A + D_B)\nabla_{\mathbf{r}} \cdot (\nabla_{\mathbf{r}} - \mathbf{F}(\mathbf{r})) \\ \times p_2^{\mathbf{r}}(\mathbf{r}, t|\mathbf{r}_0, t_0), |\mathbf{r}| \geq \sigma. \end{aligned} \quad (16)$$

Eqn. 15 describes the free diffusive motion of the coordinate \mathbf{R} . The solution of that equation, for the initial condition $p_2^{\mathbf{R}}(\mathbf{R}, t_0|\mathbf{R}_0, t_0) = \delta(\mathbf{R} - \mathbf{R}_0)$ and boundary condition $p_2^{\mathbf{R}}(|\mathbf{R}| \rightarrow \infty, t|\mathbf{R}_0, t_0) = 0$, is

$$p_2^{\mathbf{R}}(\mathbf{R}, t|\mathbf{R}_0, t_0) = \frac{\exp\left[-\frac{|\mathbf{R}-\mathbf{R}_0|^2}{4(D_A+D_B)(t-t_0)}\right]}{[4\pi(D_A+D_B)(t-t_0)]^{3/2}}. \quad (17)$$

The non-trivial solution is that of the Smoluchowski equation for the inter-particle vector \mathbf{r} . This solution also has to take into account the reactions between A and B . We will incorporate the reaction as a boundary condition on the solution of the Smoluchowski equation. To be more explicit, the initial condition and boundary conditions for the coordinate \mathbf{r} are given by

$$p_2^{\mathbf{r}}(\mathbf{r}, t_0|\mathbf{r}_0, t_0) = \delta(\mathbf{r} - \mathbf{r}_0), \quad (18)$$

$$p_2^{\mathbf{r}}(|\mathbf{r}| \rightarrow \infty, t|\mathbf{r}_0, t_0) = 0, \quad (19)$$

$$\begin{aligned} -j(\sigma, t|\mathbf{r}_0, t_0) \equiv 4\pi\sigma^2 D \left(\frac{\partial}{\partial r} - \mathbf{F}(\mathbf{r}) \right) \\ \times p_2^{\mathbf{r}}(\mathbf{r}, t|\mathbf{r}_0, t_0)|_{|\mathbf{r}|=\sigma}, \\ = k_a p_2^{\mathbf{r}}(|\mathbf{r}| = \sigma, t|\mathbf{r}_0, t_0), \end{aligned} \quad (20)$$

where ∂/∂_r denotes a derivative with respect to the interparticle separation r . It is seen that the reaction enters the problem as a third boundary condition on the solution of the Smoluchowski equation. Here $j(\sigma, t|\mathbf{r}_0, t_0)$ is the outward radial flux of probability $p_2^{\mathbf{r}}(\mathbf{r}, t|\mathbf{r}_0, t_0)$ through the “contact” surface of area $4\pi\sigma^2$. The boundary condition, also known as a *radiation* boundary condition [11, 12], states that this radial flux of probability equals the intrinsic rate constant times the probability that the particles A and B are, in fact, in contact. In the limit $k_a \rightarrow \infty$, the radiation boundary condition reduces to an *absorbing* boundary condition $p_2^{\mathbf{r}}(|\mathbf{r}| = \sigma, t|\mathbf{r}_0, t_0) = 0$, while in the limit $k_a \rightarrow 0$ the radiation boundary condition reduces to a *reflecting* boundary condition.

The Green’s function $p_2^{\mathbf{r}}(\mathbf{r}, t|\mathbf{r}_0, t_0)$ is derived in appendix A for the case in which $\mathbf{F}(\mathbf{r}) = \mathbf{0}$ for $|\mathbf{r}| > \sigma$; for cases in which $\mathbf{F}(\mathbf{r}) \neq \mathbf{0}$ for $|\mathbf{r}| > \sigma$, the Green’s functions could, depending upon the interaction potential, either be obtained analytically or numerically. Here, we will discuss some useful quantities that can be derived from the Green’s function. The first quantity of interest is the probability that a pair of particles, initially separated by \mathbf{r}_0 , survives and does not recombine by time t . This so-called *survival* probability is given by

$$S_a(t|\mathbf{r}_0, t_0) = \int_{|\mathbf{r}|>\sigma} d\mathbf{r} p_2^{\mathbf{r}}(\mathbf{r}, t|\mathbf{r}_0, t_0). \quad (21)$$

Clearly, $S_a(0|\mathbf{r}_0, t_0) = 1$ for $|\mathbf{r}_0| > \sigma$. The second quantity of interest is the reaction rate $q_a(t|\mathbf{r}_0, t_0)$, which is defined as the probability per unit time that a pair, initially separated by \mathbf{r}_0 , reacts at time t . It is related to the survival probability by

$$q_a(t|\mathbf{r}_0, t_0) \equiv -\frac{\partial S_a(t|\mathbf{r}_0, t_0)}{\partial t}. \quad (22)$$

Since the reactions are assumed to occur only at contact, the reaction rate is also given by the flux at contact

$$q_a(t|\mathbf{r}_0, t_0) = -j(\sigma, t|\mathbf{r}_0, t_0). \quad (23)$$

The above equation can also be obtained from Eq. 16 and Eq. 21 and by using the fact that the flux at $|\mathbf{r}| \rightarrow \infty$ vanishes.

The reaction rate $q_a(t|\mathbf{r}_0, t_0)$ can be interpreted as the probability that the *next* reaction for a pair of particles, initially separated by \mathbf{r}_0 , occurs at time t . This is used to set up the GFRD event-driven algorithm, which we will describe in the next section.

E. Outline of the algorithm

To explain the essence of the algorithm, it will be instructive to consider a single particle of type A that can react with a single particle of type B according to the following scheme



Furthermore, it will be useful to imagine that these particles are surrounded by neighbors, the presence of which limit the size of the time step to Δt_{\max} . As a function of time, the system will flip-flop between the associated state C and the dissociated state $A + B$. The GFRD event-driven algorithm to propagate this system would consist of iterating the following steps:

1. If the system is in the dissociated state $A + B$, then draw a next association time t according to $q_a(t|\mathbf{r}_0, t_0)$ (Eq. 22).
 - a) If $(t - t_0) \geq \Delta t_{\max}$, then the two particles will not react within the time step; new positions for A and B at time $t_0 + \Delta t_{\max}$ are obtained from $p_2^{\mathbf{R}}(\mathbf{R}, t_0 + \Delta t_{\max}|\mathbf{R}_0, t_0)$ (Eq. 17) and $p_2^{\mathbf{r}}(\mathbf{r}, t_0 + \Delta t_{\max}|\mathbf{r}_0, t_0)$ (Eq. 37) with \mathbf{R} and \mathbf{r} as given by Eqs. 10 and 11.
 - b) If $(t - t_0) < \Delta t_{\max}$, then the next reaction will occur within the time step; a new position for particle C at time t is obtained from $p_2^{\mathbf{R}}(\mathbf{R}, t|\mathbf{R}_0, t_0)$ (Eq. 17).
2. If the system is in the associated state C , then draw a next dissociation time from $q_d(t|t_0)$ (Eq. 7).
 - a) If $(t - t_0) \geq \Delta t_{\max}$, then particle C will not have decayed by $t_0 + \Delta t_{\max}$; a new position for particle C , \mathbf{r}_C , at time $t_0 + \Delta t_{\max}$ is obtained from $p_1(\mathbf{r}_C, t_0 + \Delta t_{\max}|\mathbf{r}_{C0}, t_0)$ (Eq. 5);
 - b) If $(t - t_0) < \Delta t_{\max}$, the next reaction will occur within the maximum time step; the particles A and B are placed at time t adjacent to each other at positions around \mathbf{r}_C as obtained from $p_1(\mathbf{r}_C, t|\mathbf{r}_{C0}, t_0)$ (see Eq. 5).

The procedure outlined above forms the heart of the algorithm. The crux of the method is to choose the maximum time step such that only monomolecular reactions or bimolecular reactions have to be considered. This makes it possible to use the exact solution of the Smoluchowski equation to propagate the system to the next reaction event in a single step. The full algorithm for a system of N particles thus consists of iterating the following steps:

1. Determine maximum time step Δt_{\max} . The maximum time step is determined by the condition that only single particles or pairs of particles have to be considered (see section II B and Fig. 1). For each particle i , we determine the maximum time step $\Delta t_{\max, i}$, such that it can interact with at most one other particle. The maximum global time step is then given by

$$\Delta t_{\max} = \min(\{\Delta t_{\max, i}\}). \quad (25)$$

In order to determine $\Delta t_{\max, i}$ for particle i , we assume that during that step the particle can travel at most a distance $\Delta r_{\max, i} = H\sqrt{6D_i\Delta t}$, where D_i

is the diffusion constant of particle i . We find that $H = 3$ suffices to preserve the correct steady-state distribution.

2. Determine next reaction and next reaction time.

We first construct a list of possible reactions $\{R_\nu\}$. With each reaction R_ν , we associate a survival probability function $S_\nu(t - t_0)$ and a next-reaction distribution function $q_\nu(t - t_0)$; the two are related via $q_\nu(t - t_0) = -\partial S_\nu(t - t_0)/\partial t$. For the bimolecular reactions, $q_\nu(t - t_0) = q_a(t|\mathbf{r}_0, t_0)$ as given by Eq. 22 and $S_\nu(t - t_0) = S_a(t|\mathbf{r}_0, t_0)$ as given by Eq. 21. For the monomolecular reactions, $q_\nu(t - t_0) = q_d(t|t_0) = k_d \exp(-k_d(t - t_0))$ and $S_\nu(t - t_0) = \exp(-k_d(t - t_0))$.

For each reaction R_ν , we generate a random number ξ_ν , uniformly distributed in the interval $0 < \xi_\nu < 1$. If $\xi_\nu \leq (1 - S_\nu(\infty))$, a tentative next reaction time Δt_ν is obtained from

$$\xi_\nu = \int_0^{\Delta t_\nu} q_\nu(t') dt' = 1 - S_\nu(\Delta t_\nu). \quad (26)$$

If, however, $\xi_\nu > (1 - S_\nu(\infty))$, then the reaction R_ν does not occur and it is dropped from the list of possible reactions. From the remaining list of tentative reactions, we choose as the actual next reaction the one that occurs first, *provided* that this reaction occurs within the maximum time step Δt_{\max} . Accordingly, the system will be propagated through a time Δt as given by

$$\Delta t = \min(\{\Delta t_\nu\}, \Delta t_{\max}). \quad (27)$$

Note that if there is no tentative reaction for which the tentative next reaction time $\Delta t_\nu < \Delta t_{\max}$, then no reaction will occur within the time step. Here, we also mention for completeness that for association reactions $S_\nu(\infty) \neq 0$: for two particles, that can diffuse and react subject to the boundary condition Eq. 19, there is a finite probability that they *never* react; this is related to the well-known fact that a random walker, that starts at the origin, can “escape” and never return to the origin.

3. Propagate particles. The single particles are propagated according to $p_1(\mathbf{r}, t|\mathbf{r}_0, t_0)$ in Eq. 5; if a particle decays, then the products are placed next to each other at positions centered around \mathbf{r} . For each pair of particles, the following two substeps are executed: 1) a new position for the coordinate \mathbf{R} is obtained from Eq. 17; 2) if the pair has not reacted, a new inter-particle vector \mathbf{r} is obtained from $p_2^*(\mathbf{r}, t|\mathbf{r}_0, t_0)$ in Eq. 37; else, if it has reacted, the products are placed adjacent to each other at positions around \mathbf{R} .
4. Update particles. Update identities of particles according to the executed reaction. Delete or add particles created or destroyed in that reaction.

A proof of the algorithm is given in appendix B.

Finally, we remark that the assumptions made above, namely that particles are spherical in shape and move by (free) diffusion, are not essential. An event-driven algorithm of this type could be set up in the case of non-spherical particles, interacting particles and/or those moving by other mechanisms than diffusion such as active transport. In these cases, the required Green’s functions could be obtained numerically if necessary.

III. RESULTS

This section is organized as follows: first we study a simple bimolecular reaction to show that GFRD accurately reproduces theoretical results. Then we turn our attention to a very simple model of gene expression as a typical example of a system that is well handled by the GFRD technique. We specifically focus on the levels of noise in protein concentrations and find dramatic differences between GFRD and results from the chemical master equation, that ignores spatial fluctuations. Finally we compare the performance of GFRD to a conventional Brownian Dynamics algorithm.

A. Bimolecular reaction

To test the validity of our approach, we study the reversible bimolecular reaction



with forward rate constant k_a and backward rate constant k_d . As a first test of our algorithm, we focus on an *isolated* pair of particles A and B . We use a set up in which particle A , with diameter σ , is placed at the origin and held fixed during the simulation. The second particle B , also with diameter σ , is initially placed at random in a spherical shell of radius r_0 centered around particle A . We then propagate particle B for a time t_{sim} . During this time, particle B can diffuse freely with a diffusion constant D and it can associate with particle A with a rate constant k_a and dissociate from it with a rate constant k_d . Typically, particle B will associate with and dissociate from A a (large) number of times during the simulation. We repeat this whole procedure many times. This allows us to calculate the distribution function $p_{\text{rev}}(r, t|r_0, t_0)$, which gives the probability that the two particles A and B , separated by a distance r_0 at time t_0 , are a distance r apart at a later time t . This numerical result can be compared to the analytical solution recently derived by Kim and Shin for the *reversible* reaction shown in Eq. 28 [10].

If the next reaction time were larger than the simulation time, t_{sim} , then we could in principle directly propagate the particles through t_{sim} . However, this would not

provide a stringent test of our algorithm. At each step, we therefore choose a maximum time step Δt_{\max} at random from the interval $[10^{-4}\tau, t_{\text{sim}}]$, where $\tau = \sigma^2/D$ is the unit of time. This could be interpreted as mimicking the constraint on the maximum time step arising from the presence of other particles.

Figure 2 shows excellent agreement for $p_{\text{rev}}(r, t|r_0, t_0)$ between theory and simulation for $r_0 = \sigma$. We find similar agreement between theory and simulation for other initial distances r_0 and for other values of the diffusion constant D and reaction rates k_a and k_d . It should be realized that because the particles are initially placed at contact, many reactions can occur during the time t_{sim} . Moreover, because we divide the simulation time into smaller intervals, we must propagate the particles many times, using the Green's function for an extensive range of \mathbf{r} , $t - t_0$ and \mathbf{r}_0 . Thus, at least for the case of an isolated pair of particles, this procedure provides a thorough test of our algorithm.

Next, we want to study a more complex system in which a single particle of type A is held fixed at the center of a spherical container of radius R and is surrounded by N_B particles of type B . Particle A can again react with a particle B to form the product C according to the scheme in Eq. 28; particle C , like particle A , does not diffuse. Particles B and C do not react, although they are not allowed to overlap with each other. The excluded volume interactions between a pair of two B particles and between a pair of a B and a C particle is taken into account by using reflecting boundary conditions, i.e. by setting $k_a = 0$ in Eq. 20. We note that the requirement that the B and C particles are not allowed to overlap,

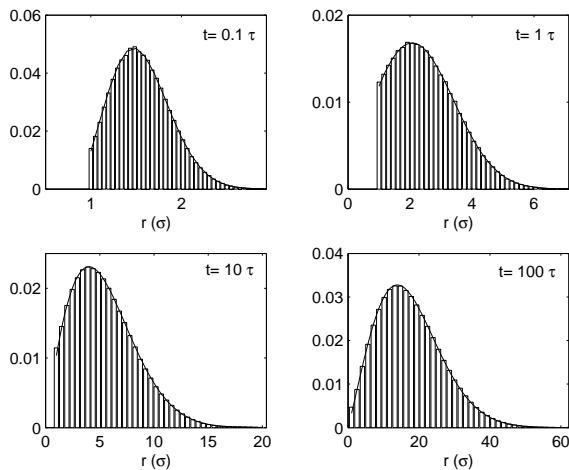


FIG. 2: The distribution $p_{\text{rev}}(r, t|\sigma, t_0 = 0)$ for $t = 0.1\tau, 1\tau, 10\tau$ and 100τ . For $r < \sigma$, the distribution $p_{\text{rev}}(r, t|\sigma, t_0) = 0$ due to the hard sphere repulsion between the particles. The bars denote the simulation results and the solid lines denote the analytical solutions of Kim and Shin [10]. Note that the particles are initially placed at contact ($r_0 = \sigma$). The forward rate constant $k_a = 1000 \text{ molecule}^{-1}\sigma^3\tau^{-1}$ and the backward rate constant is $k_d = 1\tau^{-1}$. The unit of time $\tau = \sigma^2/D$.

may impose a constraint on the maximum size of the time step, Δt_{\max} . The wall of the container is assumed to be reflecting. As no analytical solution exists for a pair of particles in the presence of a reflecting boundary, we introduce the further requirement that during a time step a particle can only interact with either the wall of the container or with another particle, but not with both.

As the B particles diffuse through the container, they will come into contact with the fixed particle A . When in contact, the particles A and B can enter the bound state C with forward rate k_a . When in the bound state, other B particles approaching the fixed C particle cannot react with it. Only after dissociation into the unbound state $A + B$, occurring at rate k_d , can another reaction occur. On average, there will be a probability p_{bound} of finding the A particle bound to the B particle. It is given by

$$p_{\text{bound}} = \frac{KN_B}{V + KN_B}, \quad (29)$$

where V is the volume available for the B particles, N_B is the total number of B particles and

$$K = g_{AB}(\sigma)k_a/k_d \quad (30)$$

is the equilibrium constant. The function $g_{AB}(r)$ is the radial distribution function for the pair of particles A and B .

The radial distribution function $g_{AB}(r)$ describes the spatial correlations arising from the interactions between the particles [13]. It is conceivable that in this system the excluded volume interactions between the particles induce spatial correlations. These correlations could affect the density of B particles that are in contact with

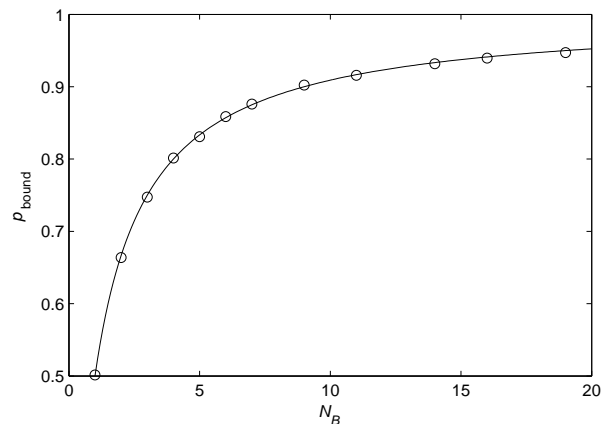


FIG. 3: The probability p_{bound} that the A particle is bound to a B particle as a function of the total number of B particles for the reaction scheme shown in Eq. 28. The symbols indicate the simulation results, while the solid line denotes the mean-field prediction (Eq. 29 with $g_{AB}(\sigma) = 1$). The radius of the container is $R = 200\sigma$ and the equilibrium constant is chosen such that it is equal to the interaction volume V . The error bars in the simulation results are smaller than the size of the symbols.

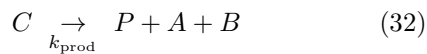
the A particle and thereby the probability that the A particle is bound to a B particle. In Eq. 30, the distribution function at contact, $g_{AB}(\sigma)$, thus describes the effect of the spatial correlations on the equilibrium constant. However, the concentrations that we consider here are very low and, as a result, the spatial correlations are expected to be small. Indeed, the simulations reveal that $g_{AB}(r) \approx 1$ for all distances r . If $g_{AB}(\sigma) = 1$, then Eqs. 29 and 30 reduce to the well-known mean-field results that can straightforwardly be obtained by solving the macroscopic rate equations in steady-state. In Fig. 3, we compare the simulation results to the mean-field prediction for p_{bound} . We find excellent agreement.

In conclusion, we have shown that our algorithm provides an accurate way of simulating an assembly of particles that can move by diffusion and react according to monomolecular and bimolecular reactions. As more complicated reactions, such as trimolecular reactions, can, in general, be decomposed into these elementary reactions, we are now in a position to simulate more complex systems.

B. Gene expression

In this section we present results for a model of gene expression. It should be stressed that the model is highly simplified. The purpose here is to show the power of our approach. Nevertheless, we find interesting effects due to the spatial fluctuations of the components that could be of relevance for more realistic systems.

The reaction network consists of the following reactions:



In Eqs. 31–33, A represents a promoter region on the DNA and B a RNA polymerase molecule that moves by free diffusion and can bind with a forward rate k_a to the promoter site to form the RNAP-DNA complex C . This complex can dissociate with a rate constant k_d . Alternatively, it can produce a protein P at a production rate k_{prod} . Proteins degrade with a decay rate k_{dec} . Note that, in this model, when a protein is produced the RNAP dissociates from the DNA.

In the living cell, the concentration of free RNAP – RNAP that is not bound to the DNA – is usually very low [15]. As a result, spatial correlations are negligible (i.e., $g_{AB}(r) = 1$) and the mean number of proteins, $\overline{N_P}$, can be obtained from the macroscopic rate equations. The result is:

$$\overline{N_P} = K_1 K_2 \frac{N_B}{V + K_1 N_B}. \quad (34)$$

Here $K_1 = k_a/(k_d + k_{\text{prod}})$ and $K_2 = k_{\text{prod}}/k_{\text{dec}}$ and N_B is the total number of B molecules.

In the simulations, we fix the promoter site, i.e. the A particle, in the center of a spherical container of radius R . The volume of the container is $V = 1\mu\text{m}^3$, which is comparable to that of the *Escherichia coli* cell. The promoter site is surrounded by $N_B = 18$ RNAP molecules, corresponding to the concentration of free RNAP of 30 nM as found in the living cell [15]. The RNAP molecules move with a diffusion constant $D = 1\mu\text{m}^2\text{s}^{-1}$, which is comparable to that of similarly sized proteins [14]. We assume that, at contact, the RNAP can associate with the promoter site at a rate as determined by the Maxwell-Boltzmann velocity distribution. This leads to $k_a = \pi\sigma^2\langle v_{AB} \rangle = 3 \cdot 10^9\text{M}^{-1}\text{s}^{-1}$, where v_{AB} is the relative velocity of the particles A and B . We note that this estimate is equal to the rate of collisions between hard spheres in the low density limit [13, 16]. We could arrive at an alternative estimate for k_a using the diffusion constant and a molecular “jump” distance λ . This would lead to $k_a = 4\pi\sigma^2 D/\lambda$. Both estimates give similar results for the value of k_a . The dissociation rate is chosen such that the equilibrium constant $K = k_a/k_d$ equals the one reported in [15], yielding $k_d = 21.5\text{s}^{-1}$. We assume that the diameters of the promoter site and the RNAP molecules are equal and given by $\sigma = 5\text{nm}$.

Here, we only simulate the promoter site and the RNAP molecules explicitly in space. The proteins are assumed to be uniformly distributed in space. Moreover, we reduce both the degradation and the production of protein molecules to single-step Poisson processes. These assumptions are unrealistic. Nevertheless, this model allows us to demonstrate the power and the flexibility of our algorithm. In particular, the production and decay reactions can simply be added to our list of possible reactions, $\{R_\nu\}$ (see section II E). The next-reaction distribution function for the production reaction is given by $q_{\text{prod}}(t) = k_{\text{prod}}N_C \exp(-k_{\text{prod}}N_C t)$, where $N_C = 0$ if the RNAP is unbound and $N_C = 1$ if it is bound to the DNA, while the propensity function for the degradation reaction is given by $q_{\text{decay}}(t) = k_{\text{decay}}N_P \exp(-k_{\text{decay}}N_P t)$. In this way, the spatially-resolved GFRD scheme can naturally be combined with kinetic Monte Carlo schemes, such as the Gillespie algorithm [6], that are based upon the spatially uniform chemical master equation.

In figure 4 we show the mean number of proteins $\overline{N_P}$ as a function of the protein production rate k_{prod} , while keeping the decay rate fixed at $k_{\text{decay}} = 0.04\text{s}^{-1}$. As the concentration of the RNAP is low and spatial correlations are expected to be negligible, the simulation results for the *average* number of proteins, $\overline{N_P}$, should follow the mean-field prediction of Eq. 34. Fig. 4 shows that this is indeed the case. However, in contrast to the mean-field analysis, the GFRD simulations allow us to quantify the effect of the *spatial fluctuations* of the RNAP molecules on the *noise* in the protein synthesis.

We can quantify the magnitude of the noise in protein

production by computing the following quantity [15]:

$$\eta_P^2 = \frac{\overline{N_P^2(t)} - \overline{N_P}^2}{\overline{N_P}^2}. \quad (35)$$

In the following analysis we have changed the degradation rate such that the average number of proteins, $\overline{N_P}$, is constant. This allows us to focus on the effect of spatial fluctuations on the noise in protein production – we thus eliminate the fairly trivial changes in the noise due to changes in the average number of proteins.

Since we are interested in the importance of spatial fluctuations in gene expression, it is natural to compare the GFRD results to those obtained using the chemical master equation. The latter approach does take into account the discrete nature of the reactants and the stochastic character of their interactions, but it treats the spatial fluctuations in a mean-field manner: at each instant, it is implicitly assumed that the particles are uniformly distributed in space. This approach is justified if there are many non-reactive collisions to stir the system in between the reactive collisions. However, the RNAP is present in low copy numbers, and, upon contact, it rapidly associates with the promoter site on the DNA. As a consequence, this reaction is diffusion-limited. This could have important implications for the noise in gene expression.

Using the techniques described in [3], we can analytically obtain the noise from the chemical master equation. It is given by

$$\eta_P^2 = \frac{1}{\overline{N_P}} - \frac{k_{\text{prod}}k_a N_B}{k_{\text{prod}}k_a N_B + \overline{N_P}(k_a N_B + k_d + k_{\text{prod}})^2}. \quad (36)$$

The first term on the right describes the result that would have been obtained if gene expression were a simple linear birth-and-death process. The second term reflects the

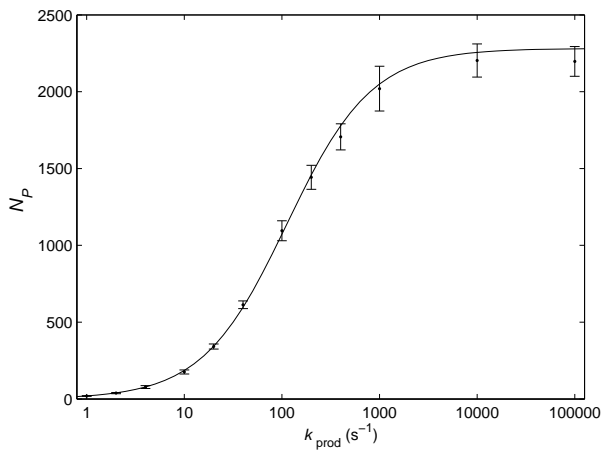


FIG. 4: The mean protein number $\overline{N_P}$ as a function of the protein production rate k_{prod} as obtained from the GFRD simulations for the reaction scheme shown in Eqs. 31 – 33. The solid line denotes the mean-field prediction given by Eq. 34.

fact that in order to produce a protein, it is necessary, albeit not sufficient, for a RNAP molecule to bind to the promoter site. This term, and thus the noise in gene expression, goes through a minimum at $k_{\text{prod}} = k_a N_B + k_d$ and vanishes for both small and large k_{prod} . In these regimes, gene expression reduces to a simple linear birth-and-death process. In the limit of small k_{prod} , the production of the protein is the rate limiting step. The RNAP molecule will associate to and dissociate from the promoter site a large number of times, before it actually induces gene expression. The former process is thus in equilibrium on the time scale of gene expression. Hence, the birth term is given by $k_{\text{birth}} = p_{\text{bound}}k_{\text{prod}}$, with p_{bound} being the probability that a RNAP molecule is bound to the promoter (see Eq. 29); the death term is given by $k_{\text{death}} = k_{\text{decay}}$. In the limit of large k_{prod} , the binding of a RNAP molecule to the promoter site is the rate limiting step: as soon as a RNAP molecule is bound to the promoter, a protein will be produced. This means that the birth term is given by $k_{\text{birth}} = k_a(1 - p_{\text{bound}})[B]$; the death term is again $k_{\text{death}} = k_{\text{decay}}$. For a linear birth-and-death process, the noise is determined by the average number of proteins, $\eta_P = 1/\sqrt{\overline{N_P}}$ [3]. As we have set the decay rate k_{decay} such that $\overline{N_P}$ is constant, the noise in gene expression must be the same in the limiting regimes of small and large k_{prod} , in which gene expression reduces to a birth-and-death process.

Figure 5 shows the noise in the protein concentration as a function of the synthesis rate for $\overline{N_P} = 1000$. The GFRD results are compared to those obtained using the chemical master equation. It is seen that for small k_{prod} both approaches yield identical results. In this regime,

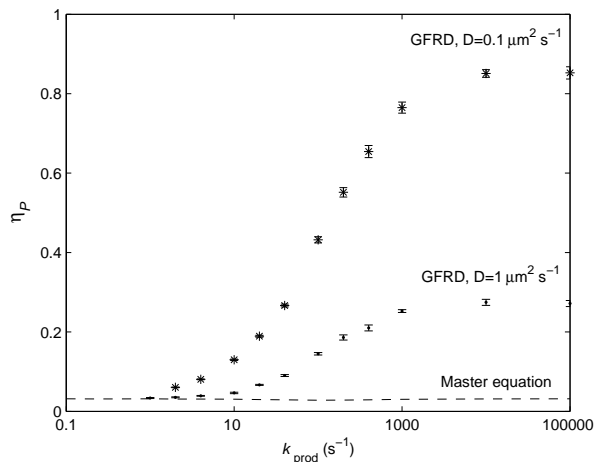


FIG. 5: The noise in protein level η_P as a function of protein production rate k_{prod} for the reaction scheme shown in Eqs. 31 – 33. Compared are the results obtained by GFRD with a diffusion constant of $D = 1\mu\text{m}^2\text{s}^{-1}$ (\cdot) and $D = 0.1\mu\text{m}^2\text{s}^{-1}$ ($*$) and the result using the chemical master equation (dashed line). The mean number of proteins was held constant at $\overline{N_P} = 1000$ by changing the degradation rate k_{decay} of the protein.

protein synthesis is the rate-limiting step. Indeed, on the time scale of gene expression the RNAP molecules have sufficient time to become well mixed in the cell. As a result, the effects of diffusion are negligible and the noise reduces to the expected value for a linear birth-and-death process.

However, for $k_{\text{prod}} \gtrsim 1\text{s}^{-1}$, spatial fluctuations can have a drastic effect on the noise in gene expression. In this regime, the noise of the spatially-resolved model is larger than that of the “well-stirred reactor” model. In fact, Fig. 5 shows that it grows fairly rapidly with increasing k_{prod} . The increase in noise is due to a very broad distribution of arrival times of RNAP molecules at the promoter site, much broader than the corresponding Poisson distribution for the system without spatial fluctuations. It is also seen that for very large production rates, the noise ultimately reaches a plateau value. At these high values of k_{prod} the promoter site becomes an “absorbing” boundary for the RNAP molecules. Fig. 5 also reveals that the height of the plateau increases as the diffusion constant D becomes smaller. This is not surprising, because the importance of spatial fluctuations is expected to be larger for smaller diffusion constants. However, it does clearly show that in order to determine the significance of spatial fluctuations in gene expression, it is of interest to establish the value of the diffusion constant of the RNA polymerase experimentally.

This model of gene expression is obviously highly simplified – our aim here is to present a new particle-based technique to simulate biochemical networks. Nevertheless, the results show that spatial fluctuations are potentially important in gene expression. Moreover, GFRD will now make it possible to study systematically how significant the effects of spatial fluctuations are on the noise in gene expression using more refined models.

C. Performance

The essence of the GFRD scheme is to exploit the analytical solution of the Smoluchowski equation for a pair of interacting particles to set up an event-driven algorithm. This allows GFRD to make large jumps in time when the particles are far apart from each other. Clearly, the performance of the algorithm depends on the density of the system: the further the particles are apart, the larger the time step that can be used and the better GFRD will perform in comparison to brute-force Brownian Dynamics schemes (see section IIA). It is thus of interest to compare the distribution of propagation times in GFRD to the time step used in a brute-force Brownian Dynamics scheme as a function of density.

In figure 6 we show the distribution of propagation times Δt for the bimolecular reaction described in section III A as a function of density. For $N_B = 18$ ($[B] = 30$ nM), the value used in the above models of gene expression, the distribution has a maximum at $\Delta t = 1 \cdot 10^{-4}$ s. The propagation times become smaller if the density in-

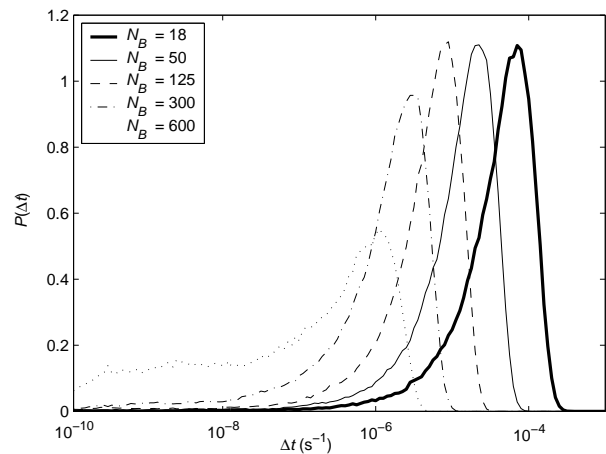


FIG. 6: The distribution of propagation times Δt for a system consisting of a single particle A in the center of a spherical box of volume $V = 1\mu\text{m}^3$, surrounded by N_B particles B ; the particles A and B can react according to a bimolecular reaction scheme (see Eq. 28). The distributions are shown for $N_B = 18$ (bold solid line), $N_B = 50$ (solid line), $N_B = 125$ (dashed line), $N_B = 300$ (dashed-dotted line) and $N_B = 600$ (dotted line), corresponding to a concentration of $[B] = 30$ nM, $[B] = 83$ nM, $[B] = 210$ nM, $[B] = 500$ nM, and $[B] = 1000$ nM, respectively. In the GFRD simulations, we use a lower cut-off for the propagation time, $2.5 \cdot 10^{-10}$ s, which corresponds to the time step used in a brute-force Brownian Dynamics simulation.

creases. For $[B] = 1\mu\text{M}$, the peak in the distribution shifts to $\Delta t = 1 \cdot 10^{-6}$ s.

In biochemical networks, the concentrations of the components can be very low. In gene networks, for example, the concentrations of the gene regulatory proteins are often in the nM regime. In signal transduction networks, the concentrations of the components may also be fairly low, i.e. in the μM range. The analysis presented here suggests that with GFRD it should be possible to reach time steps of at least $10^{-6} - 10^{-4}$ s for such networks. In contrast, in a brute-force Brownian Dynamics simulation, we cannot use a time step larger than $10^{-10} - 10^{-9}$ s ($10^{-5} - 10^{-4}\sigma^2/D$) in order to preserve the correct distribution (as, for instance, defined by the requirement that the analytical solution for the Green’s function $p_{\text{rev}}(\mathbf{r}, t|\mathbf{r}_0, t_0)$ as shown in Fig. 2 can be accurately reproduced). We thus believe that under biologically relevant conditions, GFRD can be three to six orders of magnitude faster than conventional particle-based schemes for simulating biochemical networks in time and space.

IV. CONCLUSIONS

We have developed a new technique, called Green’s Function Reaction Dynamics, to simulate biochemical networks at the particle level and in both time and space.

The main idea of the technique is to choose a maximum time step such that only single particles or pairs of particles have to be considered. For these particles, the Smoluchowski equation can be solved analytically using Green's functions. The analytical solution can then be used to set up an event-driven algorithm, quite analogous to the kinetic Monte Carlo schemes as originally developed by Bortz, Kalos and Lebowitz [19] to simulate Ising spin systems and by Gillespie to numerically solve the chemical master equation [6]. We would like to stress, however, that in contrast to the widely used "Gillespie" algorithm, our technique makes it possible to simulate biochemical networks at the particle level and in both time and *space*.

The analysis presented in section III C shows that GFRD is highly efficient. This should make it possible to simulate biochemical networks at much larger length and time scales than hitherto possible. In addition, we believe that the scheme has the potential to be even more efficient. In the current scheme, we use a global maximum time step that pertains to all particles in the system. It seems natural, however, to assign to each particle an individual maximum time step. In such a scheme, each particle would have its own individual clock. This approach would make it possible to devote most computational effort to those particles that interact frequently; the particles that are initially far from other particles are only updated once the time has come when they have a reasonable chance to interact. A second possible improvement would be to exploit the low concentration of the components in another way. In the current scheme, we explicitly take into account excluded volume interactions. In fact, this often imposes a limit on the maxi-

imum time step. If the concentrations are low, however, we would expect the excluded volume effects to be negligible for the behavior of the network. In future work, we will show how these observations can be incorporated into the algorithm to even further enhance the performance of Green's Function Reaction Dynamics.

Acknowledgments

We would like to thank Marco Morelli, Siebe van Albada and Daan Frenkel for useful discussions and suggestions and Rosalind Allen and Bela Mulder for a critical reading of the manuscript. The work is part of the research program of the "Stichting voor Fundamenteel Onderzoek der Materie (FOM)", which is financially supported by the "Nederlandse organisatie voor Wetenschappelijk Onderzoek (NWO)".

Appendix A: Solution of Smoluchowski equation

Here we consider a pair of particles A and B that move by free diffusion, but, upon contact, can react with a rate constant k_a . The Green's function $p_2^{\mathbf{r}}(\mathbf{r}, t | \mathbf{r}_0, t_0)$ for this pair can be obtained by exploiting the analogy between the diffusion of particles and the conduction of heat in solids. The corresponding Green's function for the conduction of heat in solids is derived in [11]. The Green's function $p_2^{\mathbf{r}}(\mathbf{r}, t | \mathbf{r}_0, t_0)$ is

$$p_2^{\mathbf{r}}(r, \theta, \phi, t | r_0) = \frac{1}{4\pi\sqrt{rr_0}} \sum_{n=0}^{\infty} (2n+1) P_n(\cos\theta) \int_0^{\infty} e^{-Du^2t} F_{n+1/2}(ur) F_{n+1/2}(ur_0) u du, \quad (37)$$

where

$$F_{\nu}(ur) = \frac{(2\sigma k_a + 1)[J_{\nu}(ur)Y_{\nu}(u\sigma) - Y_{\nu}(ur)J_{\nu}(u\sigma)] - 2u\sigma[J_{\nu}(ur)Y'_{\nu}(u\sigma) - Y_{\nu}(ur)J'_{\nu}(u\sigma)]}{[(2\sigma k_a + 1)J_{\nu}(u\sigma) - 2u\sigma J'_{\nu}(u\sigma)]^2 + [(2\sigma k_a + 1)Y_{\nu}(u\sigma) - 2u\sigma Y'_{\nu}(u\sigma)]^2}^{1/2}, \quad (38)$$

and where P_n is the n th Legendre polynomial, J_n and Y_n are the n th Bessel function of the first and the second kind, $D = D_A + D_B$ is the total diffusion constant of the two particles A and B and $\sigma = (d_A + d_B)/2$, where d_A and d_B are the diameters of the particles A and B , respectively; here, and below, we take $t_0 = 0$. The Green's function can be expressed in a more compact notation by

$$p_2^{\mathbf{r}}(r, \theta, \phi, t | r_0) = \sum_{n=0}^{\infty} C_n P_n(\cos\theta) R_n(r, t). \quad (39)$$

The probability $f(r | r_0, t)$ of finding the particles separated by a distance between r and $r + dr$ at time t is given by

$$f(r | r_0, t) = 2\pi \sum_{n=0}^{\infty} C_n Q_n(\pi) r^2 R_n(r, t), \quad (40)$$

with

$$Q_n(\theta) = \int_0^{\theta} \sin\theta P_n(\cos\theta) d\theta. \quad (41)$$

The conditional probability $g(\theta | r, r_0, t)$ that two particles are at an angle between θ and $\theta + d\theta$ with respect to

the original direction $\mathbf{r}_0 = \mathbf{r}_B - \mathbf{r}_A$, given that they are separated by a distance r at time t , is

$$g(\theta|r, r_0, t) = 2\pi \sum_{n=0}^{\infty} C_n Q'_n(\theta) r^2 R_n(r, t). \quad (42)$$

The survival probability $S(t)$ is given by

$$S(t) = \int_{\sigma}^{\infty} f(r|r_0, t) dr. \quad (43)$$

The above integral is complicated but it follows from the properties of the diffusion equation that it must be identical to the familiar survival probability for the spherically symmetric case [10, 17].

The above distribution functions suggest a straightforward procedure for drawing a new position \mathbf{r} from the Green's function $p_2^{\mathbf{r}}(\mathbf{r}, t|\mathbf{r}_0)$. We pretabulate $Q_n(\theta)$ and $R_n(r, r_0, t)$ up to a certain order N . From this we construct the probability distribution $f(r|r_0, t)$ and we draw

a new distance r from this distribution. Next, we draw θ from the distribution $g(\theta|r, r_0, t)$ and finally we choose ϕ uniformly distributed between 0 and 2π .

This procedure works well for large t . For small t , however, the above procedure becomes rather cumbersome as the number of terms N that needs to be included in order for the summations in Eqs. 40 and 42 to converge, becomes very large. The reason is that $p_2^{\mathbf{r}}(\mathbf{r}, t|\mathbf{r}_0)$ becomes a sharply peaked function around \mathbf{r}_0 for small t . However, for small t , the probability that the two particles will interact with each other, is relatively small. In other words, for small t the full solution $p_2^{\mathbf{r}}(\mathbf{r}, t|\mathbf{r}_0)$, is dominated by free diffusion. We can exploit this observation in order to reduce N by writing the Greens's function as $p_2^{\mathbf{r}}(\mathbf{r}, t|\mathbf{r}_0) = p_{\text{free}}(\mathbf{r}, t|\mathbf{r}_0) + p_{\text{corr}}(\mathbf{r}, t|\mathbf{r}_0)$, where p_{free} is the solution for free diffusion and p_{corr} is a correction term that takes into account the reacting boundary at $r = \sigma$. The free diffusion term can easily be computed from

$$p_{\text{free}}(r, \theta, \phi, t|r_0) = \frac{1}{[4\pi Dt]^{3/2}} \exp\left[-\frac{r^2 + r_0^2 - 2rr_0 \cos \theta}{4Dt}\right]. \quad (44)$$

Using the fact, that p_{free} can also be written as

$$p_{\text{free}}(r, \theta, \phi, t|r_0) = \frac{1}{4\pi\sqrt{rr_0}} \sum_{n=0}^{\infty} (2n+1) P_n(\cos \theta) \int_0^{\infty} e^{-Du^2 t} J_{n+1/2}(ur) J_{n+1/2}(ur_0) u du, \quad (45)$$

we find by comparison with Eq. 37 that p_{corr} can be expressed as

$$p_{\text{corr}}(r, \theta, \phi, t|r_0) = -\frac{1}{4\pi\sqrt{rr_0}} \sum_{n=0}^{\infty} (2n+1) P_n(\cos \theta) \int_0^{\infty} e^{-Du^2 t} \frac{R_1}{R_1^2 + R_2^2} (R_1 F_1 + R_2 F_2) u du, \quad (46)$$

where

$$R_1 = (2\sigma k_a + 1) J_{n+\frac{1}{2}}(u\sigma) - 2u\sigma J'_{n+\frac{1}{2}}(u\sigma), \quad (47)$$

$$R_2 = (2\sigma k_a + 1) Y_{n+\frac{1}{2}}(u\sigma) - 2u\sigma Y'_{n+\frac{1}{2}}(u\sigma), \quad (48)$$

$$F_1 = J_{n+\frac{1}{2}}(ur) J_{n+\frac{1}{2}}(ur_0) - Y_{n+\frac{1}{2}}(ur) Y_{n+\frac{1}{2}}(ur_0), \quad (49)$$

$$F_2 = J_{n+\frac{1}{2}}(ur) Y_{n+\frac{1}{2}}(ur_0) + J_{n+\frac{1}{2}}(ur_0) Y_{n+\frac{1}{2}}(ur). \quad (50)$$

As the correction term p_{corr} is usually rather small for small t , the number of terms N that needs to be included in order to compute the functions $f(r, |r_0, t)$ and $g(\theta|r, r_0, t)$, is strongly reduced.

Appendix B: Proof of the algorithm

Let $P(t, \mu)dt$ be the probability that the next reaction will occur in the time interval between t and $t + dt$ and will be reaction R_{μ} . As described in section II B, the time

step is chosen such that the reactions occur *independently* from each other. The probability $P(t, \mu)dt$ is therefore given by

$$P(t, \mu)dt = q_{\mu}(t)dt \prod_{\substack{\nu=1 \\ \nu \neq \mu}}^M S_{\nu}(t). \quad (51)$$

The algorithm features a maximum time step. It is thus conceivable that not a single reaction occurs within a time step. The probability $Q(\Delta t_{\text{max}})$ that no reaction occurs within a time step of size Δt_{max} is given by

$$Q(\Delta t_{\text{max}}) = \prod_{\nu=1}^M S_{\nu}(\Delta t_{\text{max}}). \quad (52)$$

It can easily be shown that the procedure outlined in section II E is consistent with Eqs. 51 and 52. Let $\tilde{Q}(\Delta t_{\text{max}})$ be the probability that the procedure described above does not yield a reaction within the time

step of size Δt_{\max} . It is given by

$$\check{Q}(\Delta t_{\max}) = \text{Prob}(t_\nu > \Delta t_{\max} \text{ for all } \nu) \quad (53)$$

$$= \prod_{\nu=1}^M \text{Prob}(\xi_\nu > (1 - S_\nu(\Delta t_{\max}))) \quad (54)$$

$$= \prod_{\nu=1}^M S_\nu(\Delta t_{\max}) \quad (55)$$

$$= Q(\Delta t_{\max}). \quad (56)$$

Similarly, let $\check{P}(t, \mu)dt$ be the probability that the above described procedure yields, at time t , reaction R_μ as the next reaction. It is given by

$$\begin{aligned} \check{P}(t, \mu)dt &= \text{Prob}(t < t_\mu < t + dt) \\ &\quad \times \text{Prob}(t_\nu > t_\mu \text{ for all } \nu \neq \mu) \end{aligned} \quad (57)$$

$$= q_\mu(t)dt \prod_{\substack{\nu=1 \\ \nu \neq \mu}}^M \text{Prob}(\xi_\nu > (1 - S_\nu(t_\mu))) \quad (58)$$

$$= q_\mu(t)dt \prod_{\substack{\nu=1 \\ \nu \neq \mu}}^M S_\nu(t_\mu) \quad (59)$$

$$= P(t, \mu)dt. \quad (60)$$

- [1] McAdams and A. Arkin, Proc. Natl. Acad. Sci. USA, **94**, 814 (1997).
- [2] M. B. Elowitz and S. Leibler, Nature (London) **403**, 335 (2000); N. Barkai and S. Leibler, Nature (London), **403**, 267 (2000).
- [3] N. G. van Kampen, *Stochastic Processes in Physics and Chemistry*, North-Holland, Amsterdam (1992).
- [4] Y. Togashi and K. Kaneko, Phys. Rev. Lett **86**, 2459 (2001).
- [5] N. M. Shnerb, Y. Louzoun, E. Bettelheim and S. Solomon, Proc. Natl. Acad. Sci. **97**, 10322 (2000).
- [6] D. T. Gillespie, J. Comput. Phys. **22**, 403 (1976); D. T. Gillespie, J. Phys. Chem. **81**, 2340 (1977).
- [7] C. J. Morton-Firth and D. Bray, J. Theor. Biol. **192**, 117 (1998).
- [8] B. Alberts, D. Bray, J. Lewis, M. Raff, J. Lewis, M. Raff, K. Roberts, and J. D. Watson, *Molecular Biology of the Cell*, Garland Publishing, New York, (1994).
- [9] M. Smoluchowski, Z. Phys. Chem. **92**, 129 (1917); S. Chandrasekhar, Rev. Mod. Phys. **15**, 1 (1943).
- [10] H. Kim and K. J. Shin, Phys. Rev. Lett. **82**, 1578 (1999).
- [11] H. S. Carslaw and J. C. Jaeger, *Conduction of Heat in Solids*, Oxford University Press, New York(1959).
- [12] N. Agmon, A. Szabo, J. Chem. Phys. **92**, 5270 (1990).
- [13] J.-P. Hansen & I. R. McDonald, *Theory of simple liquids*, 2nd edn, Academic Press, San Diego (1986).
- [14] M. B. Elowitz, M. G. Surette, P.-E. Wolf, J. B. Stock, and S. Leibler, J. Bacteriol. **181**, 197 (1999).
- [15] P. S. Swain, M. B. Elowitz and E. D. Siggia, Proc. Natl. Acad. Sci. **99**, 12795 (2002).
- [16] H. X. Zhou and A. Szabo, J. Chem. Phys. **95**, 5948 (1991).
- [17] S. A. Rice, *Diffusion Limited Reactions*, Elsevier Science Publishing, New York (1985).
- [18] M. Ptashne & A. Gann *Genes and signals*. Cold Spring Harbor Laboratory Press, New York (2002).
- [19] A. B. Bortz, M. H. Kalos, and J. L. Lebowitz, J. Comp. Phys. **17**, 10 (1975).